

Effect of Fractional Order on Energy Ratios at the Boundary Surface of Elastic-Piezothermoelastic Media

Rajneesh Kumar^a and Poonam Sharma*

Department of Mathematics, Kurukshetra University, Kurukshetra 136119, Haryana, India

(Received June 28, 2015, Revised October 16, 2016, Accepted November 30, 2016)

Abstract. In the present investigation reflection and transmission of plane waves at an elastic half space and piezothermoelastic solid half space with fractional order derivative is discussed. The piezothermoelastic solid half space is assumed to have 6 mm type symmetry and assumed to be loaded with an elastic half space. It is found that the amplitude ratios of various reflected and refracted waves are functions of angle of incidence, frequency of incident wave and are influenced by the piezothermoelastic properties of media. The expressions of amplitude ratios and energy ratios are obtained in closed form. The energy ratios are computed numerically using amplitude ratios for a particular model of graphite and Cadmium Selenide (CdSe). The variations of energy ratios with angle of incidence are shown graphically. The conservation of energy across the interface is verified. Some cases of interest are also deduced from the present investigation.

Keywords: reflection; piezothermoelastic; fractional order; transmission; elastic; amplitude ratios

1. Introduction

The nature of the earth is not known exactly; therefore one has to take the different mathematical model for the purpose of theoretical investigations. Abd-alla and Alsheikh (2009) studied a problem of reflection and refraction of quasi-longitudinal waves under initial stresses at an interface of two anisotropic piezoelectric media with different properties. Abd-alla *et al.* (2012) discussed propagation of plane vertical transverse waves at an interface of a semi-infinite piezoelectric elastic medium under the influence of the initial stresses. Achenbach (1973) analysed the wave propagation in elastic solids. Scott (1996) investigated the energy and dissipation of inhomogeneous plane waves in thermoelasticity.

In classical theory of thermoelasticity, Fourier's heat conduction theory assumes that the thermal disturbances propagate at infinite speed which is unrealistic from the physical point of view. One of the generalizations of the classical theory of thermoelasticity have been developed which predict only finite velocity of propagation for heat and displacement fields given by Lord and Shulman (1967) which incorporates a flux rate term into the Fourier's law of heat conduction and formulates a generalized theory admitting finite speed for thermal signals. Lord and Shulman

*Corresponding author, E-mail: poonamattri189@gmail.com

^aPh.D., E-mail: rajneesh_kuk@rediffmail.com

(1967) theory of generalized thermoelasticity have been further extended to homogeneous anisotropic heat conducting materials recommended by Dhaliwal and Sherief (1980). All these theories predict a finite speed of heat propagation. Chandrashekhariah (1986) refers to this wave-like thermal disturbance as second sound. A survey article of various representative theories in the range of generalized thermoelasticity have been brought out by Hetnarski and Ignaczak (1999).

A stressed state of a piezoelectric body is produced mainly by its deformation, as well as by thermal and electric fields present in the body. Therefore a mathematical model piezothermoelasticity quite adequately reflects the properties of such bodies. The theory of thermopiezoelectric material was first proposed by Mindlin (1974) and derived governing equations of a thermopiezoelectric plate. The physical laws for the thermopiezoelectric material have been explored by Nowacki (1978, 1979). Chandrasekharaiah (1984) used generalised Mindlin's theory of thermopiezoelectricity to account for the finite speed of propagation of thermal disturbances. Majhi (1995) studied the transient thermal response of the semi-infinite piezoelectric rod subjected to the heat source. Rao and Sunar (1993) pointed out the temperature variation in the piezoelectric media. Chen (2000) derived the general solution for transversely isotropic piezothermoelastic media. Vashishth and Sukhija (2014) investigated the problem of inhomogeneous waves at the boundary of an anisotropic piezothermoelastic medium. Othman *et al.* (2015) studied the propagation of plane waves in generalised piezothermoelastic medium: comparison of different theories. Vashishth and Sukhija (2015) studied the reflection and transmission of plane waves from a fluid-piezothermoelastic solid interface.

Fractional Calculus is a field of mathematic study that grows out of the traditional definitions of the calculus integral and derivative operators in much the same way fractional exponents is an outgrowth of exponents with integer value. Studied over the intervening three hundred years have proven at least half right. It is clear, that within the 20th century, especially numerous applications have been found. However these applications and mathematical background surrounding fractional calculus are far from paradoxical. While the physical meaning is difficult to grasp, the definitions are no more rigorous than integer order counterpart. Kumar and Gupta (2013) studied the plane wave propagation in an anisotropic thermoelastic medium with fractional order derivative and void. Bassiory and Sabry (2013) discussed the fractional order two temperature thermo-elastic behaviour of piezoelectric materials. Attenuated fractional wave equations in anisotropic media are studied by Meerschaert and McGough (2014). Sur and Kanoria (2014) discussed the fractional heat conduction with finite wave speed in a thermo-visco-elastic spherical shell. Meral and Royston (2009) investigated the response of the fractional order on viscoelastic halfspace to surface and subsurface sources. Meral *et al.* (2011) discussed the Rayleigh-Lamb wave propagation on a fractional order viscoelastic plate.

The investigation of models of an elastic and piezothermoelastic with fractional order parameter has been taken into account with growing interest under the influence of various physical fields such as thermal, electric and fractional order. An impetus for such studies was the creation of many new materials possessing properties that are not characteristic of usual elastic bodies. A piezothermoelastic half-space (PTHS), having 6 mm symmetry, loaded with elastic half-space (EHS), is considered, and the expressions for the amplitude ratios are obtained. Further, these amplitude ratios are used to compute the energy ratios corresponding to reflected and transmitted waves using the appropriate boundary conditions. The effects of the angle of incidence and the fractional order parameter on the reflected and transmitted energy ratios are observed for a particular model of graphite and Cadmium Selenide (CdSe). Some particular cases of interest are also discussed.

2. Basic equations

Following Kuang (2010) and Sherief *et al.* (2010), the basic equations for a homogeneous, anisotropic, thermally conducting, piezoelectric elastic medium in the absence of body forces and free charge density are as follows

Constitutive equations

$$\sigma_{ij} = c_{ijkl} \varepsilon_{kl} - \eta_{ijk} E_k - \beta_{ij} T, \quad (1)$$

$$D_i = \epsilon_{ij} E_j + \eta_{ijk} \varepsilon_{jk} + p_i T, \quad (2)$$

$$E_i = -\phi_{,i}, \quad (i, j, k, l = 1, 2, 3) \quad (3)$$

Equations of motion

$$\sigma_{ij,j} - \rho \ddot{u}_i = 0, \quad (4)$$

Equations of heat conduction

$$K_{ij} T_{,ij} - \left(\frac{\partial}{\partial t} + \tau_0 \frac{\partial^{\alpha+1}}{\partial t^{\alpha+1}} \right) (\rho C_e T + \beta_{ij} u_{i,j} T_0 - p_i \phi_{,i} T_0) = 0, \quad (5)$$

Gauss equation

$$D_{i,i} = 0 \quad (i, j = 1, 2, 3) \quad (6)$$

Following Achenbach (1973), the constitutive relations for the elastic half space are

$$\sigma_{ij,j}^e = 2\mu^e u_{i,j}^e + \lambda^e u_{k,k}^e \delta_{ij}, \quad (i, j, k, l = 1, 2, 3) \quad (7)$$

and, equations of motion are

$$\mu^e u_{i,jj}^e + (\lambda^e + \mu^e) u_{i,ij}^e - \rho^e \ddot{u}_i^e = 0, \quad (i, j = 1, 2, 3) \quad (8)$$

where c_{ijkl} are elastic parameters, β_{ij} are tensors of thermal moduli respectively. ρ , C_e are, respectively, the density and specific heat at constant strain, T_0 is the reference temperature, τ_0 is the thermal relaxation time, which will ensure that the heat conduction equation will predict finite speeds of heat propagation of matter from one medium to other. u_i, u_i^e are the components of displacement vectors \mathbf{u} , \mathbf{u}^e in the piezothermoelastic solid and elastic half spaces, $\sigma_{ij} (= \sigma_{ji})$, σ_{ij}^e and $\varepsilon_{ij} = \frac{1}{2}(u_{i,j} + u_{j,i})$, ε_{ij}^e are the components of the stress and strain tensor in the piezothermoelastic and elastic half spaces, $K_{ij} (= K_{ji})$ are the components of thermal conductivity, α is the fractional order such that $0 < \alpha \leq 1$, E_i is the electric field intensity, D_i is the electric displacement, ϕ is the electric potential, p_i are the pyroelectric constants, T is the absolute temperature of the medium, β_{ij} , p_i , η_{ijk} , ϵ_{ij} are tensors of piezothermal moduli, ρ^e , λ^e and μ^e are the density and the Lamé's constants in elastic media, respectively. The subscripts preceded by

comma “,” and superposed dot “.” corresponds to partial and time derivatives, respectively. The piezothermal coefficients c_{ijkl} , K_{ij} , p_i and C_e are positive.

3. Formulation of the problem

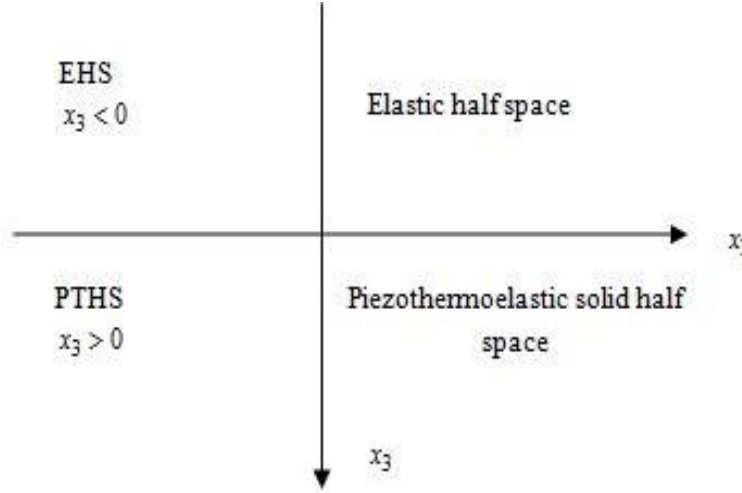


Fig. 1 Geometry of the problem

Consider a piezothermoelastic half space (PTHS), having 6 mm symmetry in welded contact with an elastic half space (EHS) (Fig. 1) in order that the PTHS occupies the region $x_3 > 0$, and the EHS occupies region $x_3 < 0$ and $x_3 = 0$ is the boundary interface. We consider plane waves in the x_1 - x_3 plane with wavefront parallel to the x_2 axis. For two dimensional problem, the displacement vectors \mathbf{u} , \mathbf{u}^e in the piezothermoelastic solid and elastic half spaces are taken as $\mathbf{u} = (u_1, 0, u_3)$ and $\mathbf{u}^e = (u_1^e, 0, u_3^e)$.

The constitutive relations for the transversely isotropic piezothermoelastic half space in the x_1 - x_3 plane are

$$\begin{aligned}
 \sigma_{11} &= c_{11}u_{1,1} + c_{13}u_{3,3} + \eta_{31}\phi_{,3} - \beta_{11}T, \\
 \sigma_{13} &= c_{44}(u_{1,3} + u_{3,1}) + \eta_{15}\phi_{,1}, \\
 \sigma_{33} &= c_{13}u_{1,1} + c_{33}u_{3,3} + \eta_{33}\phi_{,3} - \beta_{33}T, \\
 D_1 &= \eta_{15}(u_{1,3} + u_{3,1}) - \epsilon_{11}\phi_{,1}, \\
 D_3 &= \eta_{31}u_{1,1} + \eta_{33}u_{3,3} - \epsilon_{33}\phi_{,3} + p_3T, \\
 E_1 &= -\phi_{,1}, \\
 E_3 &= -\phi_{,3},
 \end{aligned} \tag{9a}$$

The constitutive relations for the elastic half space in the x_1 - x_3 plane are

$$\begin{aligned}
 \sigma_{11}^e &= \mu^e (u_{1,3}^e + u_{3,1}^e) + \lambda^e (u_{1,1}^e + u_{3,3}^e), \\
 \sigma_{33}^e &= \mu^e (u_{3,1}^e + u_{1,3}^e) + \lambda^e (u_{1,1}^e + u_{3,3}^e),
 \end{aligned} \tag{9b}$$

The field equations for transversely isotropic piezothermoelastic medium are

$$\left. \begin{aligned} c_{11}u_{1,11} + c_{13}u_{3,31} + \eta_{31}\phi_{,31} - \beta_{11}T_{,1} + c_{44}(u_{1,33} + u_{3,13}) + \eta_{15}\phi_{,13} &= \rho\ddot{u}_1, \\ c_{13}u_{1,13} + c_{33}u_{3,33} + \eta_{33}\phi_{,33} - \beta_{33}T_{,3} + c_{44}(u_{1,31} + u_{3,11}) + \eta_{15}\phi_{,11} &= \rho\ddot{u}_3, \\ K_{11}T_{,11} + K_{33}T_{,33} - \left(\frac{\partial}{\partial t} + \tau_0 \frac{\partial^{\alpha+1}}{\partial t^{\alpha+1}} \right) (\rho C_e T + T_0\beta_{11}u_{1,1} + T_0\beta_{33}u_{3,3} - T_0p_3\phi_{,3}) &= 0, \\ \eta_{15}(u_{1,31} + u_{3,11}) - \epsilon_{11}\phi_{,11} + \eta_{31}u_{1,13} + \eta_{33}u_{3,33} - \epsilon_{33}\phi_{,33} + p_3T_{,3} &= 0, \end{aligned} \right\} \quad (10a)$$

And the field equations for the elastic half space are

$$\left. \begin{aligned} \mu^e(u_{1,11}^e + u_{1,33}^e) + (\lambda^e + \mu^e)u_{3,13}^e - \rho^e\ddot{u}_1^e &= 0, \\ \mu^e(u_{3,11}^e + u_{3,33}^e) + (\lambda^e + \mu^e)u_{1,31}^e - \rho^e\ddot{u}_3^e &= 0, \end{aligned} \right\} \quad (10b)$$

We introduce the following dimensionless quantities

$$\begin{aligned} (x_1', x_3', u_1', u_3', u_1^e', u_3^e') &= \frac{\omega_1}{c_1} (x_1, x_3, u_1, u_3, u_1^e, u_3^e), \quad (t', \tau_0') = \omega_1 (t, \tau_0), \quad T' = \frac{T}{T_0}, \\ \phi' = \frac{\phi}{\phi_0}, \quad (\sigma_{ij}', \sigma_{ij}^e') &= \frac{1}{\beta_{11}T_0} (\sigma_{ij}, \sigma_{ij}^e), \quad (P', P^e') = \frac{1}{\beta_{11}T_0c_1} (P, P^e) \end{aligned} \quad (11)$$

where

$$c_1 = \sqrt{\frac{c_{11}}{\rho}}, \quad \omega_1 = \frac{\rho C_e c_1^2}{K_{11}}$$

Using these dimensionless quantities in the Eqs. (10a) and (10b) with the removal of primes (') can be written as

$$\begin{aligned} \left(c_{11} \frac{\partial^2}{\partial x_1^2} + c_{44} \frac{\partial^2}{\partial x_3^2} - a_{11} \frac{\partial^2}{\partial t^2} \right) u_1 + a_{12} \frac{\partial^2 u_3}{\partial x_1 \partial x_3} + a_{13} \frac{\partial^2 \phi}{\partial x_1 \partial x_3} - a_{14} \frac{\partial T}{\partial x_1} &= 0, \\ a_{12} \frac{\partial^2 u_1}{\partial x_1 \partial x_3} + \left(c_{44} \frac{\partial^2}{\partial x_1^2} + c_{33} \frac{\partial^2}{\partial x_3^2} - a_{11} \frac{\partial^2}{\partial t^2} \right) u_3 + a_{15} \frac{\partial^2 \phi}{\partial x_1^2} - a_{16} \frac{\partial T}{\partial x_3} &= 0, \\ -a_{26} \frac{\partial u_1}{\partial x_1} - a_{27} \frac{\partial u_3}{\partial x_1} - a_{29} \frac{\partial \phi}{\partial x_3} + \left(K_{11} \frac{\partial^2}{\partial x_1^2} + K_{33} \frac{\partial^2}{\partial x_3^2} - m_{20} \right) T &= 0, \\ a_{22} \frac{\partial^2 u_1}{\partial x_1 \partial x_3} + a_{33} \frac{\partial^2 u_3}{\partial x_3^2} - a_{24} \left(\frac{\partial^2}{\partial x_1^2} + \frac{\partial^2}{\partial x_3^2} \right) \phi + a_{25} \frac{\partial T}{\partial x_3} &= 0, \end{aligned} \quad (12)$$

$$\begin{aligned} \left(\frac{\alpha^e - \beta^e}{c_1^2} \right) \left(\frac{\partial^2 u_1^e}{\partial x_1^2} + \frac{\partial^2 u_3^e}{\partial x_3 \partial x_1} \right) + \frac{\beta^e}{c_1^2} \left(\frac{\partial^2 u_1^e}{\partial x_1^2} + \frac{\partial^2 u_1^e}{\partial x_3^2} \right) &= \frac{\partial^2 u_1^e}{\partial t^2}, \\ \left(\frac{\alpha^e - \beta^e}{c_1^2} \right) \left(\frac{\partial^2 u_1^e}{\partial x_3 \partial x_1} + \frac{\partial^2 u_3^e}{\partial x_3^2} \right) + \frac{\beta^e}{c_1^2} \left(\frac{\partial^2 u_3^e}{\partial x_1^2} + \frac{\partial^2 u_3^e}{\partial x_3^2} \right) &= \frac{\partial^2 u_3^e}{\partial t^2}, \end{aligned}$$

where $\alpha^e = \sqrt{\frac{\lambda^e + 2\mu^e}{\rho^e}}$, $\beta^e = \sqrt{\frac{\mu^e}{\rho^e}}$ are velocities of longitudinal and transverse waves respectively. The displacement components are written as

$$u_1^e = \frac{\partial \phi^e}{\partial x_1} - \frac{\partial \psi^e}{\partial x_3}, \quad u_3^e = \frac{\partial \phi^e}{\partial x_3} + \frac{\partial \psi^e}{\partial x_1}, \quad (13)$$

where ϕ^e and ψ^e are scalar potentials which satisfy the following wave equations

$$\nabla^2 \phi^e = \frac{\ddot{\phi}^e}{\alpha^2}, \quad \nabla^2 \psi^e = \frac{\ddot{\psi}^e}{\beta^2}, \quad (14)$$

Where

$$\alpha' = \frac{\alpha^e}{c_1}, \quad \beta' = \frac{\beta^e}{c_1}.$$

The notations used above are mentioned in the Appendix A. For plane harmonic waves, we assume the wave solution in the piezothermoelastic medium is of the form

$$(u_1, u_3, \phi, T) = (U, A, B, C) \exp \left[i\omega \left(-\frac{x_1}{c} - qx_3 + t \right) \right] \quad (15)$$

where ω is the circular frequency and q is the unknown slowness parameter, c is the apparent phase velocity U , A , B and C are the unknown amplitude vectors associated with harmonic wave and that are independent of time t and coordinates x_1 , x_3 . The system of Eq. (12), with the aid of Eq. (15), yield a system

$$\mathbf{VS} = 0, \quad (16)$$

where $S=[U,A,B,C]^T$, and \mathbf{V} is a 4×4 matrix whose elements are listed in Appendix A. This system of the equations has a non-trivial solution if the determinant of the coefficients $S=[U,A,B,C]^T$ vanish i.e.,

$$\det \mathbf{V} = 0, \quad (17)$$

which yields a characteristic equation in q as

$$f_{11}q^8 + f_{12}q^6 + f_{13}q^4 + f_{14}q^2 + f_{15} = 0 \quad (18)$$

The coefficients $f_{1i}(i=1,2,3,4,5)$ are given in Appendix A. q_1, q_2, q_3 and q_4 correspond to the roots of the Eq. (18) whose imaginary parts are positive, and q_5, q_6, q_7 and q_8 denote the roots whose imaginary parts are negative. The eigen values are arranged in descending order such that q_1, q_2 and q_3 corresponds to the propagating quasi P (qP) mode, quasi S (qS) mode, quasi T (qT) mode and q_4 corresponds to the electric potential component wave mode (eP) of wave propagation, respectively.

The complex phase velocities of the quasi-waves, given by $v_i = \frac{n_i}{q_i}$, $i = 1, 2, 3$, where n_i

represents the direction of slowness, will be varying with the direction of phase propagation. The complex velocity of the quasi-waves, i.e., $v_i = v_{Ri} + iv_{Ii}$, defines the phase propagation velocity $V_i = \frac{v_{Ri}^2 + v_{Ii}^2}{v_{Ri}}$, and attenuation quality factor $Q_i^{-1} = \frac{\text{Img}(1/v_i^2)}{\text{Re}(1/v_i^2)}$ for the corresponding waves.

For each q_i ($i=1,2,\dots,8$), the corresponding eigen vectors U_i, A_i, B_i and C_i can be written as

$$W_i = \frac{\text{cof}(V_{42})_{q_i}}{\text{cof}(V_{41})_{q_i}}, \Phi_i = \frac{\text{cof}(V_{43})_{q_i}}{\text{cof}(V_{41})_{q_i}}, \Theta_i = \frac{\text{cof}(V_{44})_{q_i}}{\text{cof}(V_{41})_{q_i}}, \quad (19)$$

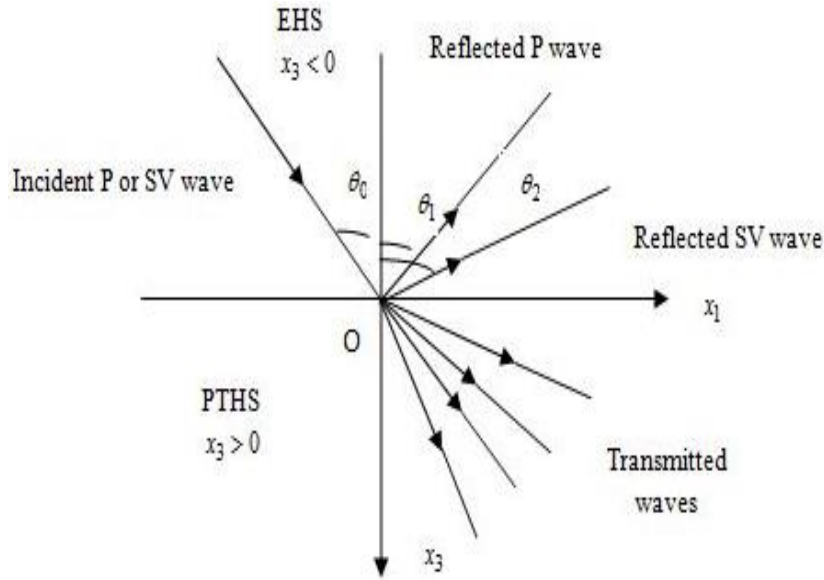


Fig. 2 Reflection and transmission of plane wave in PTHS with EHS

where

$$W_i = \frac{A_i}{U_i}, \Phi_i = \frac{B_i}{U_i}, \Theta_i = \frac{C_i}{U_i}, \quad (20)$$

and $\text{cof}(V_{ij})_{q_i}$ denotes the cofactor of V_{ij} to the eigen value q_i . The amplitudes (U_i, A_i, B_i and C_i) of the plane harmonic waves decrease as these waves propagates in a piezothermoelastic medium. The amplitudes of the plane harmonic waves propagating in a piezothermoelastic medium also depend on the frequency. The formal solution for the mechanical displacement and the electric potential becomes

$$(u_1, u_3, \phi, T) = \sum_{i=1}^8 (1, W_i, \Phi_i, \Theta_i) U_i \exp\left(i\omega\left(-\frac{x_1}{c} - q_i x_3 + t\right)\right), \quad (21)$$

The solution of wave in the elastic medium can be expressed as

$$\left. \begin{aligned} \phi^e &= A_0^e e^{\left[\frac{i\omega(-x_1 \sin \theta_0 - x_3 \cos \theta_0)}{\alpha'} + t \right]} + A_1^e e^{\left[\frac{i\omega(-x_1 \sin \theta_0 + x_3 \cos \theta_0)}{\alpha'} + t \right]}, \\ \psi^e &= B_0^e e^{\left[\frac{i\omega(-x_1 \sin \theta_0 - x_3 \cos \theta_0)}{\beta'} + t \right]} + B_1^e e^{\left[\frac{i\omega(-x_1 \sin \theta_0 + x_3 \cos \theta_0)}{\beta'} + t \right]}, \end{aligned} \right\} \quad (22)$$

where A_0^e (B_0^e) and are amplitudes of the incident P(or SV) wave and, A_1^e and B_1^e are amplitudes of reflected P wave and reflected SV wave, respectively.

4. Reflection and transmission coefficients

4.1 Amplitude ratios

A plane longitudinal wave, making an angle θ_0 with the x_3 axis is incident at the interface through the EHS. This wave results in one reflected longitudinal wave (P wave) and one reflected transverse wave (SV wave) in the EHS and four transmitted waves, represented by qP, qS, qT corresponds to the quasi-longitudinal, quasi-transverse, quasi-thermal and the fourth mode eP corresponds to the electric potential wave mode in the PTHS.

The formal solutions for the mechanical displacements, the temperature, the electric potential, the stress components, and the electric displacements in a PTHS are

$$\left. \begin{aligned} (u_1, u_3, \phi, T) &= \sum_i (1, W_i, \Phi_i, \Theta_i) U_i \exp \left\{ i\omega \left(-\frac{x_1}{c} - qx_3 + t \right) \right\}, \\ (\sigma_{33}, \sigma_{31}, D_3) &= i\omega \sum_i (D_{1i}, D_{2i}, D_{4i}) U_i \exp \left\{ i\omega \left(-\frac{x_1}{c} - qx_3 + t \right) \right\}, \end{aligned} \right\} \quad (23)$$

where $c = \frac{V_0}{\sin \theta_0}$ and $V_0 = \begin{cases} \alpha' & \text{for incident P wave} \\ \beta' & \text{for incident SV wave} \end{cases}$

The coefficients D_{1i} , D_{2i} and D_{4i} have been computed and are mentioned in appendix B.

The formal solution of wave in elastic medium is given by Eq. (22).

The boundary conditions at the interface $x_3=0$ are as follows:

(i) Continuity of normal stress

$$\sigma_{33} = \sigma_{33}^e, \quad (24a)$$

(ii) Continuity of the tangential stress

$$\sigma_{13} = \sigma_{13}^e, \quad (24b)$$

(iii) Continuity of tangential displacement

$$u_1 = u_1^e, \quad (24c)$$

(iv) Continuity of normal displacement

$$u_3 = u_3^e, \tag{24d}$$

(v) Thermally insulated boundary

$$\frac{\partial T}{\partial x_3} = 0, \tag{24e}$$

(vi) Vanishing of electric displacement

$$D_3 = 0, \tag{24f}$$

Eqs. (21)-(22) with the aid of Eqs. (12)-(14) and these boundary conditions result into a non-homogeneous system

$$AX = B, \tag{25}$$

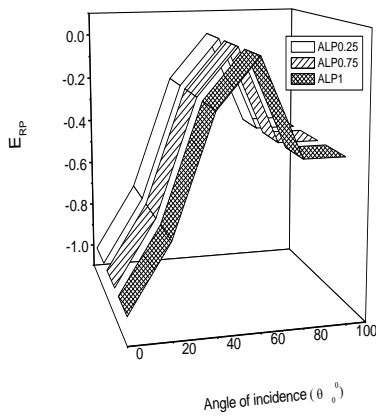


Fig. 3 Variation of reflected energy ratio (E_{RP}) with angle of incidence (P wave)

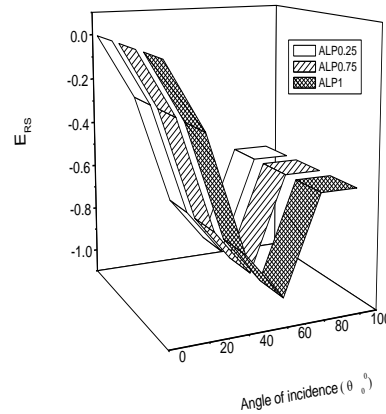


Fig. 4 Variation of reflected energy ratio (E_{RS}) with angle of incidence (SV wave)

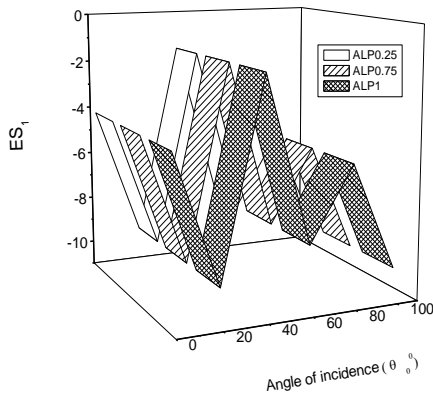


Fig. 5 Variation of transmitted energy ratio (ES_1) with angle of incidence (Transmitted qP)

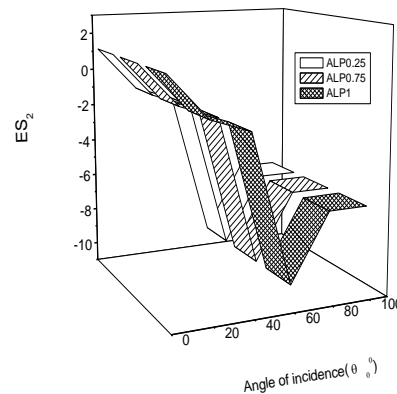


Fig. 6 Variation of transmitted energy ratio (ES_2) with angle of incidence (Transmitted qS)

where

$$A = \begin{pmatrix} D_{11} & D_{12} & D_{13} & D_{14} & D_{15} & D_{16} \\ D_{21} & D_{22} & D_{23} & D_{24} & D_{25} & D_{26} \\ D_{31} & D_{32} & D_{33} & D_{34} & D_{35} & D_{36} \\ D_{41} & D_{42} & D_{43} & D_{44} & D_{45} & D_{46} \\ D_{51} & D_{52} & D_{53} & D_{54} & 0 & 0 \\ D_{61} & D_{62} & D_{63} & D_{64} & 0 & 0 \end{pmatrix},$$

$$\mathbf{X} = [X_1, X_2, X_3, X_4, X_5^e, X_6^e]^T, \quad \mathbf{B} = [N_1, N_2, N_3, N_4, 0, 0]^T,$$

and the elements of 6×6 matrix A and notations used in \mathbf{X} and \mathbf{B} are given in the Appendix B. After solving the system Eq. (25), the transmitted and the reflected amplitude ratios are obtained.

4.2 Energy ratios

The distribution of energy between different reflected and transmitted waves at the interface $x_3=0$, across a surface element of unit area is considered. Following Scott (1996), Kuang and Yuan (2011) and Ikeda (1996), the normal acoustic flux P in a piezothermoelastic solid is

$$P = -\text{Re} \left(\sigma_{31} \bar{u}_1 + \sigma_{33} \bar{u}_3 - \phi \bar{D}_3 + K_{33} \bar{T}_{,3} \frac{T}{T_0} \right). \quad (26)$$

and for incident and reflected waves for the elastic phase are

$$P^e = -\text{Re}(\sigma_{31}^e \dot{u}_1^e + \sigma_{33}^e \dot{u}_3^e), \quad (27)$$

The average energy fluxes of the incident waves are

$$\langle P_{IP}^e \rangle = \frac{1}{2\alpha'} \omega^4 \rho^e c_1^2 \cos \theta_0 |A_0^e|^2, \quad \langle P_{IS}^e \rangle = \frac{1}{2\beta'} \omega^4 \rho^e c_1^2 \cos \theta_0 |B_0^e|^2, \quad (28)$$

and the average energy fluxes of the reflected waves are

$$\langle P_{RP}^e \rangle = -\frac{1}{2\alpha'} \omega^4 \rho^e c_1^2 \text{Re}(\cos \theta_1) |A_1^e|^2, \quad \langle P_{RS}^e \rangle = -\frac{1}{2\beta'} \omega^4 \rho^e c_1^2 \text{Re}(\cos \theta_2) |B_1^e|^2, \quad (29)$$

and the average energy fluxes of the transmitted waves are derived as

$$\langle P_s \rangle = \frac{1}{2} \omega^2 \text{Re} \left(D_{2s} + D_{1s} \bar{W}_s + \bar{D}_{4s} \Phi_s + \frac{i}{\omega} \frac{K_{33}}{T_0} \bar{D}_{5s} \Theta_s \right) |X_s|^2, \quad (s=1, 2, 3, 4) \quad (30)$$

The energy ratios of the reflected and transmitted waves are defined as

(i) For incident P wave

$$E_{RP} = \frac{\langle P_{RP}^e \rangle}{\langle P_{IP}^e \rangle}, E_{RS} = \frac{\langle P_{RS}^e \rangle}{\langle P_{IP}^e \rangle}, ES_s = \frac{\langle P_s \rangle}{\langle P_{IP}^e \rangle}, (s=1,2,3,4) \tag{31}$$

(ii) For incident SV wave

$$E_{RP} = \frac{\langle P_{RP}^e \rangle}{\langle P_{IS}^e \rangle}, E_{RS} = \frac{\langle P_{RS}^e \rangle}{\langle P_{IS}^e \rangle}, ES_s = \frac{\langle P_s \rangle}{\langle P_{IS}^e \rangle}, (s=1,2,3,4) \tag{32}$$

The interaction energy ratios in the both cases, which account for the interaction between different fields and displacements corresponding to transmitted waves, are described as

$$E_{st} = \frac{\langle P_{st} \rangle}{\langle P_{IP}^e \rangle}, \text{ for incident P wave.}$$

$$E_{st} = \frac{\langle P_{st} \rangle}{\langle P_{IS}^e \rangle}, \text{ for incident SV wave.}$$

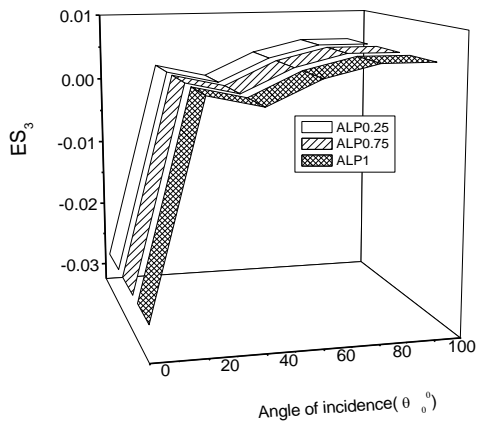


Fig. 7 Variation of transmitted energy ratio (ES_3) with angle of incidence (Transmitted qT)

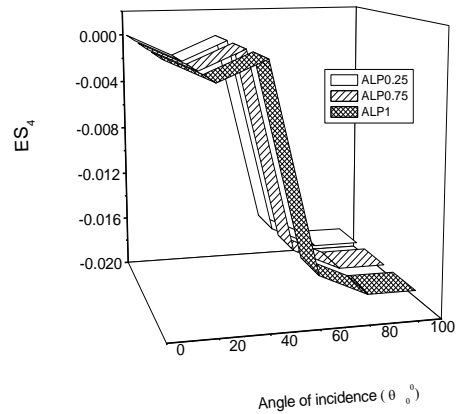


Fig. 8 Variation of transmitted energy ratio (ES_4) with angle of incidence (Transmitted eP)

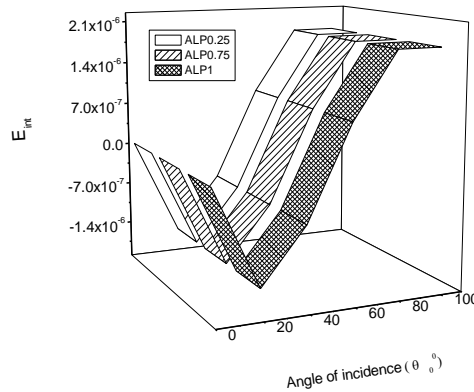


Fig. 9 Variation of interaction energy ratio (E_{int}) with angle of incidence

where

$$\langle P_{st} \rangle = \frac{1}{2} \omega^2 \operatorname{Re} \left(D_{2s} U_s \bar{U}_t + D_{1s} \bar{W}_t U_s \bar{U}_t + \bar{D}_{4s} \Phi_t U_t \bar{U}_s + \frac{i K_{33}}{\omega T_0} \bar{D}_{5s} \Theta_s \bar{U}_s U_t \right), (s=1,2,3,4) \quad (33)$$

The energy is conserved if

$$\sum_{s=1}^4 E S_s + E_{\text{int}} + E_{RP} + E_{RS} = 1, \quad (34)$$

where $E_{\text{int}} = \sum_{\substack{s,t=1 \\ s \neq t}}^4 E_{st}$ is the resultant interaction energy between the transmitted waves.

5. Numerical discussion

The amplitude ratios and energy ratios for the reflected and transmitted waves and the interaction energy ratios are computed numerically with the help of the software Matlab 7.8 and graphs of energy ratios are shown. Further, law of conservation of energy is verified.

Following Vashishth and Sukhija (2015), we take the following values of the piezothermoelastic parameters.

$$\begin{aligned} c_{11} &= 7.41 \text{ GPa}, \quad \eta_{13} = -0.160 \text{ Cm}^{-2}, \quad \beta_{11} = 0.621 \times 10^6 \text{ PaK}^{-1}, \quad \tau_0 = 0.02 \text{ s}, \\ c_{12} &= 45.2 \text{ GPa}, \quad \eta_{33} = 0.347 \text{ Cm}^{-2}, \quad \beta_{33} = 0.551 \times 10^6 \text{ PaK}^{-1}, \quad C_e = 260 \text{ JKg}^{-1} \text{ K}^{-1}, \\ c_{13} &= 39.3 \text{ GPa}, \quad \eta_{51} = -0.138 \text{ Cm}^{-2}, \quad K_{11} = 9 \text{ WK}^{-1} \text{ m}^{-1}, \quad \omega = 100 \text{ Hz}, \\ c_{33} &= 83.6 \text{ GPa}, \quad \epsilon_{11} = 8.26 \times 10^{-11} \text{ Fm}^{-1}, \quad K_{33} = 9 \text{ WK}^{-1} \text{ m}^{-1}, \quad \rho = 5504 \text{ Kgm}^{-3}, \\ c_{44} &= 13.2 \text{ GPa}, \quad \epsilon_{33} = 9.03 \times 10^{-11} \text{ Fm}^{-1}, \quad T_0 = 298 \text{ K}, \quad p_3 = -2.94 \times 10^{-6} \text{ CK}^{-1} \text{ m}^{-2}. \end{aligned}$$

Following Bullen (1963), the numerical data of graphite in elastic medium is given by $\alpha^e = 5.27 \times 10^3 \text{ ms}^{-1}$, $\rho^e = 2.65 \times 10^3 \text{ Kgm}^{-3}$, $\beta^e = 3.17 \times 10^3 \text{ ms}^{-1}$.

In all the graphs, notations \square ALP 0.25, ▨ ALP 0.75, ▩ ALP 1 denote the energy ratio curves corresponding the value of fractional order parameter at $\alpha=0.25, 0.75$ and $\alpha=1$, respectively.

5.1 For incident P wave

5.1.1 Energy ratios of reflected wave (E_{RP})

It is noticed that Fig. 3 depicts the energy ratio for the reflected P wave monotonically increases with increase in angle of incidence from 0° to 60° . Then it decreases for the angle of incidence varying from 60° to 80° and for $80^\circ \leq \theta_0 \leq 100^\circ$, it becomes stationary for the different values of fractional order parameter.

5.1.2 Energy ratios of reflected wave (E_{RS})

It is noticed that Fig. 4 shows the energy ratio for the reflected SV wave decreases with

increase in angle of incidence from 0° to 60° . Then it instantaneous increases with the angle of incidence varying from 60° to 80° and for $80^\circ \leq \theta_0 \leq 100^\circ$, it becomes stationary. It shows the same behaviour for the different values of fractional order parameter i.e., $\alpha=0.25, 0.75, 1$.

5.1.3 Energy ratios of transmitted wave (ES_1)

The energy ratio for the transmitted wave (qP) decreases initially and near the normal incidence, it increases and for intermediate values of θ_0° , it shows the oscillating behaviour as shown in Fig. 5 for the different values of fractional order parameter.

5.1.4 Energy ratios of transmitted wave (ES_2)

Fig. 6 shows that the energy ratio for the transmitted wave (qS) decreases monotonically with increase in angle of incidence from 0° to 60° . Then it increases as θ_0° increases and for $80^\circ \leq \theta_0 \leq 100^\circ$, it becomes stationary for all values of α .

5.1.5 Energy ratios of transmitted wave (ES_3)

Fig. 7 shows that the energy ratio for the transmitted wave (qT) instantly increases with increase in angle of incidence from 0° to 20° . It is evident that it shows a moderate increment in

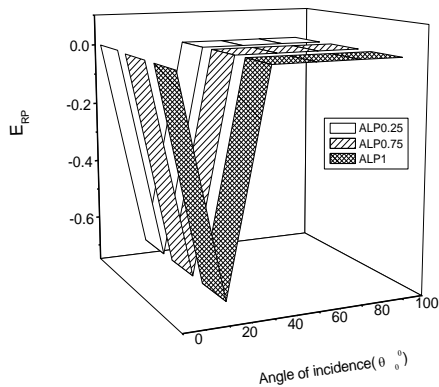


Fig. 10 Variation of reflected energy ratio with angle of incidence (P wave)

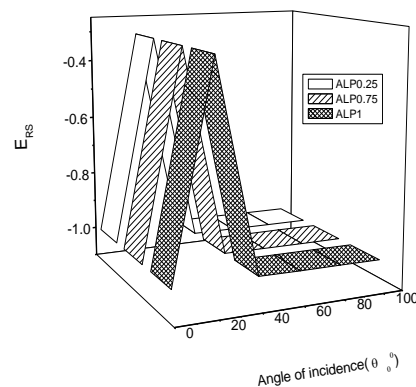


Fig. 11 Variation of reflected energy ratio with angle of incidence (SV wave)

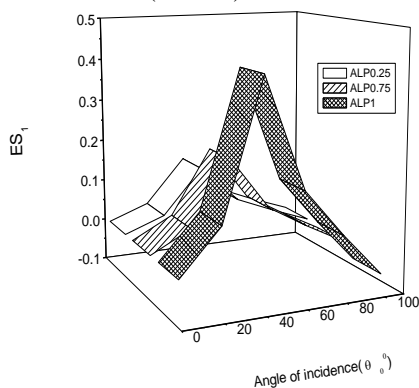


Fig. 12 Variation of transmitted energy ratio with angle of incidence (Transmitted qP)

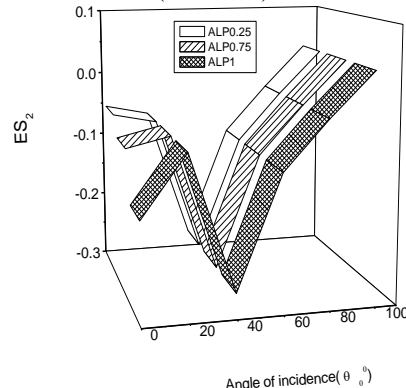


Fig. 13 Variation of transmitted energy ratio with angle of incidence (Transmitted qS)

energy ratio for θ_0° lies between 20° and 40° and it continuously decreases for $60^\circ \leq \theta_0^\circ \leq 100^\circ$ with the variations in fractional order parameter.

5.1.6 Energy ratios of transmitted wave (ES_4)

From Fig. 8, it is clear that the energy ratio for the transmitted wave (eP) decreases $0^\circ \leq \theta_0^\circ \leq 40^\circ$. Further slightly increases but then continuously decreases for $\theta_0^\circ \geq 40^\circ$ for the different values of fractional order parameter.

5.1.7 Interaction energy ratios (E_{int})

Fig. 9 shows the variations in interaction energy ratio with respect to angle of incidence for the different values of fractional order parameter. For $0^\circ \leq \theta_0^\circ \leq 20^\circ$, it decreases and the monotonically increases with increase in angle of incidence and for $80^\circ \leq \theta_0^\circ \leq 100^\circ$, it becomes stationary.

5.2 For incident SV wave

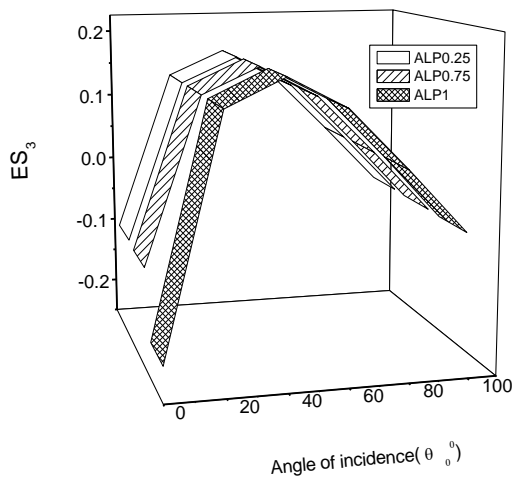


Fig. 14 Variation of transmitted energy ratio (ES_3) with angle of incidence (Transmitted qT)

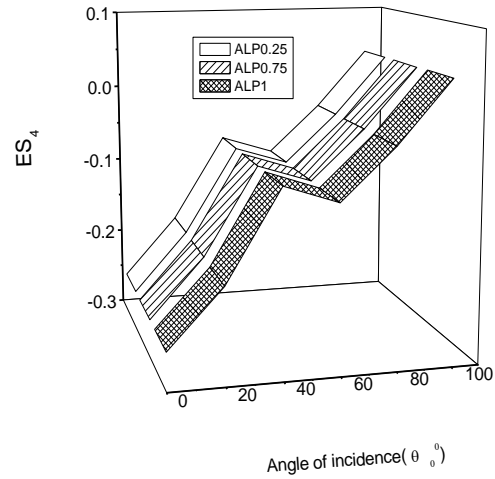


Fig. 15 Variation of transmitted energy ratio (ES_4) with angle of incidence (Transmitted eP)

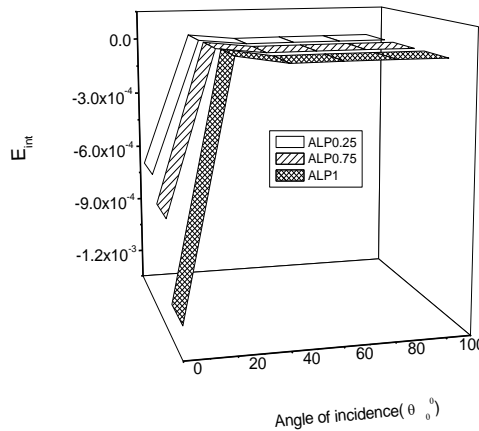


Fig. 16 Variation of interaction energy ratio (E_{int}) with angle of incidence

5.2.1 Energy ratios of reflected wave (E_{RP})

It is noticed that Fig. 10 infers the energy ratio for the reflected P wave first decreases for $0^\circ \leq \theta_0 \leq 20^\circ$ and then monotonically increases with increase in angle of incidence from 0° to 40° . Then it shows the stationary behaviour for the angle of incidence $\theta_0 \geq 40^\circ$ for the different values of fractional order parameter i.e., $\alpha=0.25, 0.75, 1$.

5.2.2 Energy ratios of reflected wave (E_{RS})

It is noticed that Fig. 11 shows the energy ratio for the reflected SV wave increases with increase in angle of incidence from 0° to 20° . Then it decreases for the angle of incidence varying from 20° to 40° . It shows the stationary behaviour for the different values of fractional order parameter i.e., $\alpha=0.25, 0.75, 1$ with increase in angle of incidence.

5.2.3 Energy ratios of transmitted wave (ES_1)

The energy ratio for the transmitted wave (qP) monotonically increases initially for $0^\circ \leq \theta_0 \leq 40^\circ$

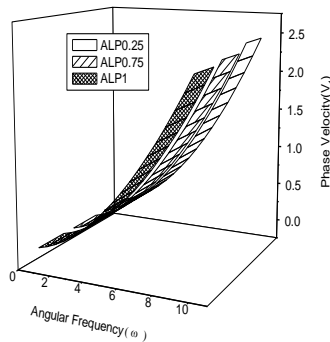


Fig. 17 Variation of phase velocity with angular frequency (quasi longitudinal wave)

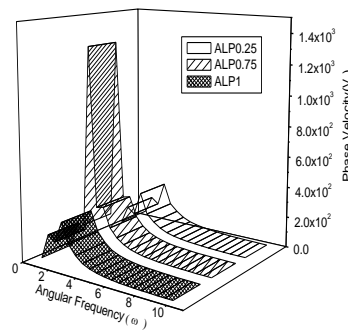


Fig. 18 Variation of phase velocity with angular frequency (quasi transverse wave)

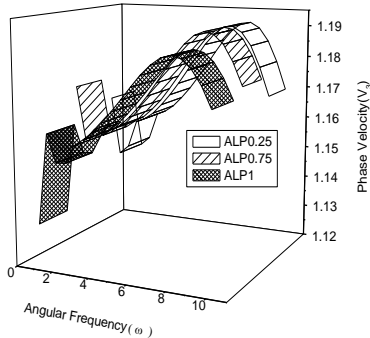


Fig. 19 Variation of phase velocity with angular frequency (quasi thermal wave)

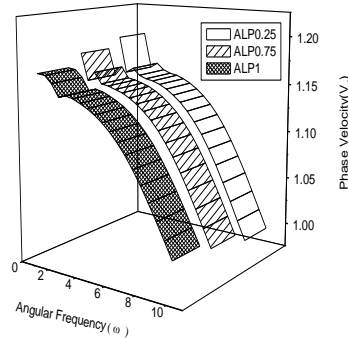


Fig. 20 Variation of phase velocity with angular frequency (electric potential wave)

and then decreases for $\theta_0 \geq 40^\circ$. At $\theta_0 \leq 40^\circ$, the magnitude values of energy ratios are in descending order for $\alpha=0.25, 0.75, 1$ as shown in Fig. 12.

5.2.4 Energy ratios of transmitted wave (ES_2)

Fig. 13 shows that the energy ratio for the transmitted wave (qS) increases with highest

magnitude value for $\alpha=0.25$, then decreases with angle of incidence varies from 20° to 40° . Then it increases for $\theta_0 \geq 40^\circ$ and onwards for $\alpha=0.25, 0.75, 1$.

5.2.5 Energy ratios of transmitted wave (ES_3)

Fig. 14 shows that the energy ratio for the transmitted wave (qT) increases for $0^\circ \leq \theta_0 \leq 40^\circ$ and then decreases with increase in angle of incidence. It is evident that the energy ratios for $\alpha=0.25, 0.75$ possess higher magnitude values than for $\alpha=1$.

5.2.6 Energy ratios of transmitted wave (ES_4)

From Fig. 15, it is clear that the energy ratio for the transmitted wave (eP) increases $0^\circ \leq \theta_0 \leq 40^\circ$ and $60^\circ \leq \theta_0 \leq 100^\circ$ but decreases for $40^\circ \leq \theta_0 \leq 60^\circ$ for the different values of fractional order parameter.

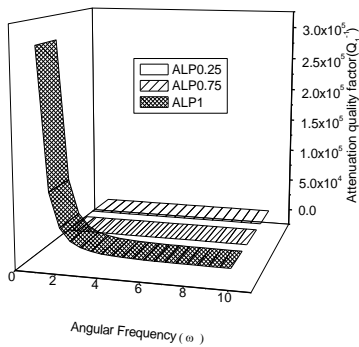


Fig. 21 Variation of attenuation quality factor with angular frequency (quasi longitudinal wave)

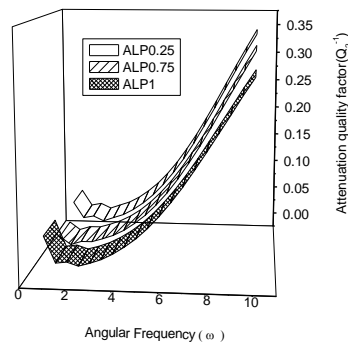


Fig. 22 Variation of attenuation quality factor with angular frequency (quasi transverse wave)

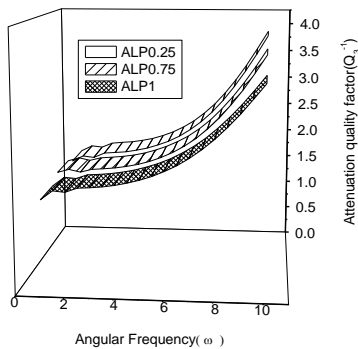


Fig. 23 Variation of attenuation quality factor with angular frequency (quasi thermal wave)

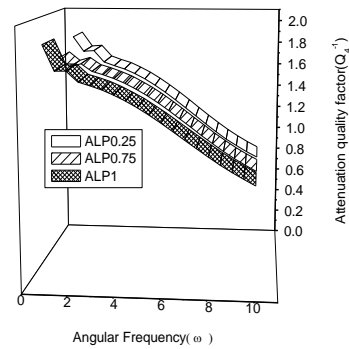


Fig. 24 Variation of attenuation quality factor with angular frequency (electric potential wave)

5.2.7 Interaction energy ratios (E_{int})

Fig. 16 shows the variations in interaction energy ratios with respect to angle of incidence which increase for $0^\circ \leq \theta_0 \leq 20^\circ$ and then become stationary. In the beginning, the values of energy ratios corresponding to $\alpha=0.25, 0.75$ are greater than value corresponding to $\alpha=1$ but further show the same behaviour with increase in angle of incidence.

5.3 Phase velocity and attenuation quality factor

Figs. 17-20 depict the variation of phase velocity (V_i) and Figs. 21-24 depict the variation of attenuation quality factor (Q_i^{-1}) of the obtained waves with respect to angular frequency (ω) for the different values of fractional order parameter and for the dimensionless value of $c(c=0.001)$ taken arbitrary and $n_1=1$. The phase velocity (V_1) of quasi longitudinal wave shows a constant behaviour of increasing trend for the different values of α . And, the phase velocity (V_2) of quasi transverse wave hikes for $\alpha=0.75$ and then shows a sudden fall depicting further the same behaviour as for the other values of α . V_3 shows an alternate behaviour but finally tends to decrease with the increase in angular frequency. And, V_4 shows the same behaviour of decreasing trend with respect to angular frequency for the different considered values of α .

The attenuation quality factor (Q_i^{-1}) first increases for $\alpha=1$, then shows a constant behaviour for $2 \leq \omega \leq 10$. Figs. 22, 23 show the increasing trend of Q_2^{-1} and Q_3^{-1} for different values of α and, Q_4^{-1} decreases with the increase in angular frequency and varying α .

6. Particular cases

- By taking $\tau_0=0$, we obtained the energy ratios at the interface of elastic and piezothermoelastic half spaces.
- If $\alpha=1$, we obtained the energy ratios at an interface of elastic and piezothermoelastic solid half spaces with one relaxation time. The results obtained are similar to one if we solve the problem directly.

7. Conclusions

- Amplitude ratios are affected by the frequency, angle of incidence fractional order parameter and piezothermoelastic properties of the material.
- Piezothermoelastic and fractional order parameter have a significant influence on the energy ratios.
- Principle of conservation of energy has been verified.
- The different values of fractional order parameter (α) depict variations in energy ratios of the different reflected and transverse waves with different magnitude values.

The effect of fractional order parameter on phase velocity and attenuation quality factor of the obtained waves has been observed ominously.

References

- Abo-el-nour, N. and Alsheikh, F.A. (2009), "Reflection and refraction of plane quasi-longitudinal waves at an interface of two piezoelectric media under initial stresses", *Arch. Appl. Mech.*, **79**(9), 843-857.
- Abo-el-nour, N., Al-sheikh, F.A. and Al-Hossain, A.Y. (2012), "The reflection phenomena of quasi-vertical transverse waves in piezoelectric medium under initial stresses", *Meccan.*, **47**(3), 731-744.
- Achenbach, J.D. (1973), *Wave Propagation in Elastic Solids*, North Holland Pub., Amsterdam, The Netherlands.

- Bassiouny, E. and Sabry, R. (2013), "Fractional order two temperature thermo-elastic behavior of piezoelectric materials", *J. Appl. Math. Phys.*, **1**(5), 110.
- Bullen, K.E. (1963), *An Introduction to the Theory of Seismology*, Cambridge University Press, U.K.
- Chandrasekharaiah, D.S. (1988), "A generalized linear thermoelasticity theory for piezoelectric media", *Acta Mech.*, **71**(1-4), 39-49.
- Chandrasekharaiah, D.S. (1986), "Thermoelasticity with second sound: A review", *Appl. Mech. Rev.*, **39**(3), 355-376.
- Chen, W.Q. (2000), "Three dimensional green's function for two-phase transversely isotropic piezothermoelastic media", *ASME J. Appl. Mech.*, **67**, 705.
- Dhaliwal, R.S. and Sherоof, H.H. (1980), "Generalized thermoelasticity for anisotropic media", *Q. Appl. Math.*, 1-8.
- Hetnarski, R.B. and Ignaczak, J. (1999), "Generalized thermoelasticity", *J. Therm. Str.*, **22**(4-5), 451-476.
- Ikeda, T. (1996), *Fundamentals of Piezoelectricity*, Oxford University Press, New York, U.S.A.
- Kuang, Z.B. (2010), "Variational principles for generalized thermodiffusion theory in pyroelectricity", *Acta Mech.*, **214**(3-4), 275-289.
- Kuang, Z.B. and Yuan, X.G. (2011), "Reflection and transmission of waves in pyroelectric and piezoelectric materials", *J. Sound Vibr.*, **330**(6), 1111-1120.
- Kumar, R. and Gupta, V. (2013), "Plane wave propagation in an anisotropic thermoelastic medium with fractional order derivative and void", *J. Thermoelast.*, **1**(1), 21-34.
- Lord, H.W. and Shulman, Y. (1967), "The generalised dynamic theory of thermoelasticity", *J. Mech. Phys. Sol.*, **15**, 299-309.
- Majhi, M.C. (1995), "Discontinuities in generalized thermoelastic wave propagation in a semi-infinite piezoelectric rod", *J. Technol. Phys.*, **36**(3), 269-278.
- Mindlin, R.D. (1974), "Equations of high frequency vibrations of thermopiezoelectric crystal plates", *J. Sol. Struct.*, **10**(6), 625-637.
- Meral, F.C. and Royston, T.J. (2009), "Surface response of a fractional order viscoelastic halfspace to surface and subsurface sources", *J. Acoust. Soc. Am.*, **126**(6), 3278-3285.
- Meral, F.C., Royston, T.J. and Magin, R.L. (2011), "Rayleigh-lamb wave propagation on a fractional order viscoelastic plate", *J. Acoust. Soc. Am.*, **129**(2), 1036-1045.
- Meerschaert, M.M. and McGough, R.J. (2014), "Attenuated fractional wave equations with anisotropy", *J. Vibr. Acoust.*, **136**(5), 050902.
- Nowacki, W. (1978), "Some general theorems of thermopiezoelectricity", *J. Therm. Str.*, **1**(2), 171-182.
- Nowacki, W. (1979), *Foundation of Linear Piezoelectricity*, Interactions in Elastic Solids, Springer, Wein.
- Othman, M.I.A., Atwa, S.Y., Hasona, W.M. and Ahmed, E.A.A. (2015), "Propagation of plane waves in generalised piezo-thermoelastic medium: Comparison of different theories", *J. Inn. Res. Sci. Eng. Technol.*, **4**(7).
- Rao, S.S. and Sunar, M. (1993), "Analysis of thermopiezoelectric sensors and actuators in advanced intelligent structures", *AIAA J.*, **31**(7), 1280-1286.
- Scott, N.H. (1996), "Energy and dissipation of inhomogeneous plane waves in thermoelasticity", *Wave Mot.*, **23**(4), 393-406.
- Sherief, H.H., El-Sayed, A.M.A. and El-Latief, A.A. (2010), "Fractional order theory of thermoelasticity", *J. Sol. Struct.*, **47**(2), 269-275.
- Sur, A. and Kanoria, M. (2014), "Fractional heat conduction with finite wave speed in a thermo-visco-elastic spherical shell", *Lat. Am. J. Sol. Struct.*, **11**(7), 1132-1162.
- Vashishth, A.K. and Sukhija, H. (2014), "Inhomogeneous waves at the boundary of an anisotropic piezothermoelastic medium", *Acta Mech.*, **225**(12), 3325-3338.
- Vashishth, A.K. and Sukhija, H. (2015), "Reflection and transmission of plane waves from fluid-piezothermoelastic solid interface", *Appl. Math. Mech.*, **36**(1), 11-36.

Appendix A

$$\begin{aligned}
V_{11} &= m_{11} - m_{12}q^2, & V_{12} &= -m_{13}q, & V_{13} &= -m_{14}q, & V_{14} &= -im_{15}q \\
V_{21} &= -m_{13}q, & V_{22} &= m_{31} - m_{23}q^2, & V_{23} &= -(m_{16} + m_{33}q^2), & V_{24} &= -im_{17}q \\
V_{31} &= -im_{12}, & V_{32} &= -im_{22}q, & V_{33} &= -im_{24}q, & V_{34} &= m_{30} - m_{19}q^2 \\
V_{41} &= m_{25}q, & V_{42} &= m_{26}q^2, & V_{43} &= m_{28} + m_{27}q^2, & V_{44} &= im_{29}q \\
f_{11} &= -m_{12}g_{11}, & f_{12} &= m_{11}g_{11} - m_{12}g_{12} + m_{13}g_{16} - m_{14}g_{18} + m_{15}g_{21}, \\
f_{13} &= m_{11}g_{12} - m_{12}g_{13} + m_{13}g_{15} - m_{14}g_{19} + m_{15}g_{21}, \\
f_{14} &= m_{11}g_{13} - m_{12}g_{14} + m_{13}g_{17} - m_{14}g_{20} + m_{15}g_{22}, & f_{15} &= m_{11}g_{14} + m_{15}g_{23}, \\
g_{11} &= -m_{23}b_{13} + m_{33}b_{14}, & g_{12} &= -m_{23}b_{11} + m_{31}b_{12} + m_{16}b_{14} + m_{33}b_{13} - m_{17}b_{16}, \\
g_{13} &= -m_{23}b_{18} + m_{31}b_{11} + m_{16}b_{13} - m_{17}b_{15}, & g_{14} &= -m_{31}b_{18}, \\
g_{15} &= -m_{13}b_{17} + m_{16}b_{20} + m_{33}b_{19} - m_{17}b_{21}, \\
g_{16} &= m_{33}b_{20}, & g_{17} &= m_{13}b_{18} + m_{16}b_{19} + m_{17}b_{22}, & g_{18} &= m_{23}b_{24} - m_{13}b_{14}, \\
g_{19} &= -m_{13}b_{19} + m_{23}b_{23} - m_{31}b_{24} - m_{17}b_{25}, & g_{20} &= -m_{31}b_{23}, \\
g_{21} &= -m_{13}b_{16} + m_{23}b_{27} - m_{33}b_{28}, & g_{22} &= -m_{13}b_{15} + m_{23}b_{26} - m_{31}b_{27} - m_{16}b_{28}, \\
g_{23} &= -m_{31}b_{26}, & b_{11} &= m_{24}m_{29} + m_{28}m_{19} - m_{30}m_{27}, & b_{12} &= m_{27}m_{19}, & b_{13} &= m_{22}m_{29} - m_{30}m_{26}, \\
b_{14} &= m_{36}m_{19}, & b_{15} &= -m_{22}m_{28}, & b_{16} &= -m_{22}m_{27} + m_{24}m_{26}, & b_{17} &= m_{24}m_{29} + m_{28}m_{19} - m_{30}m_{27}, \\
b_{18} &= -m_{30}m_{28}, & b_{19} &= m_{21}m_{29} - m_{30}m_{25}, & b_{20} &= m_{25}m_{19}, & b_{21} &= b_{27} = -m_{21}m_{27} + m_{24}m_{25}, \\
b_{22} &= m_{21}m_{28}, & b_{23} &= m_{21}m_{29} - m_{30}m_{25}, & b_{24} &= m_{19}m_{25}, \\
b_{25} &= m_{21}m_{26} - m_{22}m_{25}, & b_{26} &= -m_{21}m_{28}, & b_{28} &= -b_{25}, \\
m_{11} &= -\frac{c_{11}}{c^2} + a_{11}, & m_{12} &= c_{44}, & m_{13} &= \frac{a_{12}}{c}, & m_{14} &= \frac{a_{13}}{c}, & m_{15} &= \frac{a_{15}}{c}, & m_{16} &= \frac{a_{15}}{c^2}, & m_{17} &= \frac{a_{16}}{\omega}, \\
m_{18} &= \frac{-K_{11}}{c^2}, & m_{19} &= -K_{33}, & m_{20} &= a_{17} \left(\frac{i}{\omega} + \tau_0 \frac{(i\omega)^\alpha}{\omega} \right), & m_{21} &= \frac{a_{26}m_{20}}{c\omega}, & m_{22} &= \frac{a_{27}m_{20}}{c\omega}, \\
m_{23} &= c_{33}, & m_{24} &= \frac{a_{21}m_{20}}{\omega}, & m_{25} &= \frac{-a_{22}}{c}, & m_{26} &= -a_{23}, & m_{27} &= a_{24}, & m_{28} &= \frac{m_{20}}{c^2}, & m_{29} &= \frac{a_{25}}{\omega}, \\
m_{30} &= m_{18} - m_{20}, & m_{31} &= -\frac{c_{44}}{c^2} + a_{11}, & m_{33} &= a_{30}, & a_{11} &= \rho\omega\alpha c_1, & a_{12} &= c_{13} + c_{44}, \\
a_{13} &= (\eta_{31} + \eta_{15}) \frac{\phi_0\omega\alpha}{c_1}, & a_{14} &= \beta_{11}T_0, & a_{15} &= \eta_{15} \frac{\phi_0\omega\alpha}{c_1}, & a_{16} &= \beta_{33}T_0, \\
a_{17} &= \frac{\rho c_e c_1^2}{\alpha_1}, & a_{18} &= \frac{\beta_{11}}{\rho c_e}, & a_{19} &= \frac{\beta_{33}}{\rho c_e}, & a_{21} &= \frac{p_3\phi_0\omega\alpha}{\rho c_e T_0 c_1}, & a_{22} &= (\eta_{31} + \eta_{15}), & a_{23} &= (\eta_{33} + \eta_{15}), & a_{24} &= (c_{31}^e + c_{33}^e) \frac{\phi_0\omega\alpha}{c_1}, & a_{25} \\
a_{27} &= m_{20}a_{19}, & a_{29} &= m_{20}a_{21}, & a_{30} &= \eta_{33} \frac{\phi_0\omega\alpha}{c_1}.
\end{aligned}$$

Appendix B

$$D_{1i} = -i\omega \left((c_{33}W_i + \eta_{33}\Phi_i)q_i + \frac{c_{13}}{c} + \frac{\beta_{33}T_0\Theta_i}{i\omega} \right), \quad D_{2i} = - \left(\frac{c_{44}W_i + \left(\frac{\eta_{15}\Phi_i\phi_0\omega_1}{c_1} \right)}{c} \right) - c_{44}q_i, \quad D_{3i} = 1,$$

$$D_{4i} = W_i, \quad D_{5i} = \Theta_i q_i, \quad D_{6i} = i\omega \left(\left(-\eta_{33}W_i + \frac{\epsilon_{33}\Phi_i\phi_0\omega_1}{c_1} \right) q_i - \frac{\eta_{31}}{c} + \frac{p_3T_0\Theta_i}{i\omega} \right), \quad (i = 1, 2, 3, 4)$$

(i)For incident P wave

$$D_{15} = \omega^2 \rho^e c_1^2 \left(1 - \frac{2\beta^{e^2} \sin^2 \theta_0}{\alpha^{e^2}} \right), \quad D_{16} = -2\omega^2 \rho^e c_1^2 \sin \theta_2 \cos \theta_2, \quad D_{25} = -\frac{\beta^{e^2} \omega^2 \rho^e c_1^2 \sin 2\theta_0}{\alpha^{e^2}},$$

$$D_{26} = -\omega^2 \rho^e c_1^2 \cos 2\theta_2, \quad D_{35} = \frac{i\omega \sin \theta_0}{\alpha}, \quad D_{36} = \frac{i\omega \cos \theta_2}{\beta}, \quad D_{45} = -\frac{i\omega \cos \theta_0}{\alpha}, \quad D_{46} = \frac{i\omega \sin \theta_2}{\beta},$$

$$X_i = \frac{U_i}{A_0^e}, (i = 1, 2, 3, 4), \quad X_5 = \frac{A_1^e}{A_0^e}, \quad X_6 = \frac{B_1^e}{A_0^e}, \quad N_1 = -D_{15}, \quad N_2 = D_{25}, \quad N_3 = -D_{35}, \quad N_4 = D_{45},$$

(ii)For incident SV wave

$$D_{15} = \omega^2 \rho^e c_1^2 \left(1 - \frac{2\beta^{e^2} \sin^2 \theta_1}{\alpha^{e^2}} \right), \quad D_{16} = -2\omega^2 \rho^e c_1^2 \sin \theta_0 \cos \theta_0, \quad D_{25} = -\frac{\beta^{e^2} \omega^2 \rho^e c_1^2 \sin 2\theta_1}{\alpha^{e^2}},$$

$$D_{26} = -\omega^2 \rho^e c_1^2 \cos 2\theta_0, \quad D_{35} = \frac{i\omega \sin \theta_1}{\alpha}, \quad D_{36} = -\frac{i\omega \cos \theta_0}{\beta}, \quad D_{45} = -\frac{i\omega \cos \theta_1}{\alpha}, \quad D_{46} = \frac{i\omega \sin \theta_0}{\beta},$$

$$X_i = \frac{U_i}{B_0^e}, (i = 1, 2, 3, 4), \quad X_5 = \frac{A_1^e}{B_0^e}, \quad X_6 = \frac{B_1^e}{B_0^e}, \quad N_1 = D_{16}, \quad N_2 = -D_{26}, \quad N_3 = D_{36}, \quad N_4 = -D_{46},$$